J|A|C|S ARTICLES

Published on Web 06/03/2010

Molecular Crowding Stabilizes Folded RNA Structure by the Excluded Volume Effect

Duncan Kilburn,[†] Joon Ho Roh,[†,‡,§] Liang Guo,[||] Robert M. Briber,*[,‡] and Sarah A. Woodson*[,†]

T. C. Jenkins Department of Biophysics, Johns Hopkins University, Baltimore, Maryland 21218, Department of Materials Science and Engineering, University of Maryland, College Park, Maryland 20742, NIST Center for Neutron Research, National Institute of Standards and Technology, Gaithersburg, Maryland 20899, and BioCAT, Department of BCPS, Illinois Institute of Technology, Chicago, Illinois 60616

Received February 21, 2010; E-mail: rbriber@jhu.edu; swoodson@jhu.edu

Abstract: Crowder molecules in solution alter the equilibrium between folded and unfolded states of biological macromolecules. It is therefore critical to account for the influence of these other molecules when describing the folding of RNA inside the cell. Small angle X-ray scattering experiments are reported on a 64 kDa bacterial group I ribozyme in the presence of polyethylene-glycol 1000 (PEG-1000), a molecular crowder with an average molecular weight of 1000 Da. In agreement with expected excluded volume effects, PEG favors more compact RNA structures. First, the transition from the unfolded to the folded (more compact) state occurs at lower $MgCl_2$ concentrations in PEG. Second, the radius of gyration of the unfolded RNA decreases from 76 to 64 Å as the PEG concentration increases from 0 to 20% wt/vol. Changes to water and ion activities were measured experimentally, and theoretical models were used to evaluate the excluded volume. We conclude that the dominant influence of the PEG crowder on the folding process is the excluded volume effect.

Introduction

The folding of ribonucleic acids (RNAs) into their compact, native, form is a process whose details are the subject of much current research.[1,2] The link between structural specificity and biological function is particularly well illustrated in the case of ribozymes because their catalysis requires precise alignment of substrates, active site residues, and metal ions within the 3D folded structure of the RNA.[3] The efficient realization of that alignment by the folding of an RNA chain into a specific three-dimensional tertiary structure is essential for the proper function of a healthy cell.

It is known that cells contain up to 30% by volume of macromolecular species such as proteins, DNA, and other RNA.[4,5] This crowding affects the chemical activity of any given species, depending on the size and shape of all molecules present.[5−8] In this work, our aim was to measure the change in the folding energetics of RNA imposed by the introduction of crowder molecules into the solution.

Historically, RNA folding experiments have focused on dilute solutions with as few components as possible: RNA, dissociated cations and anions, and buffer (i.e., Tris-HCl). In such a system, the close association of cations with the RNA and the expulsion of anions reduce the electrostatic repulsion between phosphodiesters, allowing the RNA to fold.[9,10] Divalent ions like Mg^{2+} are particularly efficient in stabilizing RNA tertiary structures.[11−17] However, other species in the solution can influence the RNA's chemical potential and, therefore, change the equilibrium between folded and unfolded states. Therefore, experiments in dilute solution fail to measure other contributions to RNA stability *in vivo*, notably excluded volume effects caused by inert cosolutes.

There are a number of ways in which crowding can affect the equilibrium between unfolded and folded states of RNA. First, the chemical potential of a molecule depends on the

[†] Johns Hopkins University.
[‡] University of Maryland.
[§] National Institute of Standards and Technology.
[||] Illinois Institute of Technology.

(1) Li, P. T. X.; Vieregg, J.; Tinoco, I., Jr. *Annu. Rev. Biochem.* **2008**, *77*, 77.
(2) Woodson, S. A. *Curr. Opin. Chem. Biol.* **2005**, *9*, 104.
(3) Doudna, J. A.; Cech, T. R. *Nature* **2002**, *418*, 222.
(4) Ellis, R. J. *Trends Biochem. Sci.* **2001**, *26* (10), 597.
(5) Thirumalai, D.; Klimov, D. K.; Lorimer, G. H. *Proc. Nat. Acad. Sci. U.S.A.* **2003**, *100* (20), 11195.
(6) Minton, A. P. *Biopolymers* **1981**, *20*, 2093.
(7) Minton, A. P. *Curr. Opin. Struct. Biol.* **2000**, *10*, 34.
(8) Zhou, H.-X.; Rivas, G.; Minton, A. P. *Ann. Rev. Biophys.* **2008**, *37*, 375.
(9) Draper, D. E.; Grilley, D.; Soto, A. M. *Annu. Rev. Biomol. Struct.* **2005**, *34*, 221.
(10) Manning, G. S. *Q. Rev. Biophys.* **1978**, *11* (2), 179.
(11) Stein, A.; Crothers, D. M. *Biochemistry* **1976**, *15* (1), 160.
(12) Quigley, G. J.; Teeter, M. M.; Rich, A. *Proc. Nat. Acad. Sci. U.S.A.* **1978**, *75* (1), 64.
(13) Misra, V. K.; Draper, D. E. *Proc. Nat. Acad. Sci. U.S.A.* **2001**, *98* (22), 12456.
(14) Soto, A. M.; Misra, V. K.; Draper, D. E. *Biochemistry* **2007**, *46*, 2973.
(15) Grilley, D.; Misra, V.; Caliskan, G.; Draper, D. E. *Biochemistry* **2007**, *46*, 10266.
(16) Heilman-Miller, S. L.; Thirumalai, D.; Woodson, S. A. *J. Mol. Biol.* **2001**, *306*, 1157.
(17) Koculi, E.; Hyeon, C.; Thirumalai, D.; Woodson, S. A. *J. Am. Chem. Soc.* **2007**, *129*, 2676.

 10.1021/ja101500g

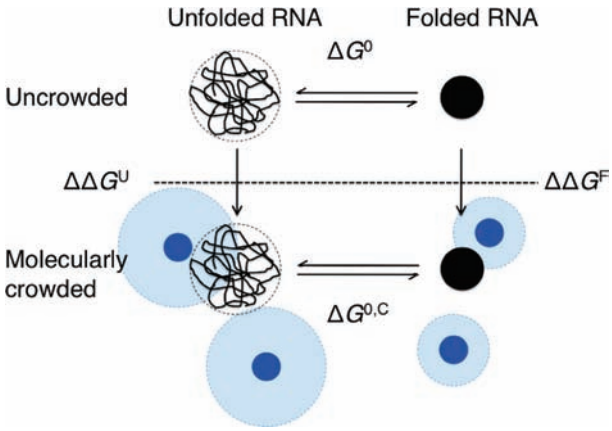

Figure 1. Molecular crowding and RNA folding. The unfolded RNA (left side) is modeled as a random coil without internal excluded volume (a Brownian walk). The dashed line around the unfolded RNA represents the effective hard particle used in eq 1, defined as a convex hull surrounding the coil that excludes volume available to all other particles in the solution.[36] The folded RNA (black circle; right side) is modeled as a hard sphere. The dark blue circles represent crowder molecules; the lighter blue "halos" represent the (RNA size-dependent) volume that is excluded to the center of gravity of the RNA molecules due to the crowders. The uppermost crowder on the unfolded side is as close to the RNA as possible; hence the center of the RNA is at the light blue halo's edge. ΔG^0 is the Gibbs free energy change for RNA folding at the standard state, defined as $\Delta G^0 = G^{F,0} - G^{U,0} = -RT \ln K^0$; $\Delta\Delta G^U = RT \ln \gamma_U$ and $\Delta\Delta G^F = RT \ln \gamma_F$ are the changes in free energies of the unfolded and folded RNA states due to the introduction of crowders, γ's defined according to eq 1; $\Delta G^{0,C} = (G^{F,0} + RT \ln \gamma_F) - (G^{U,0} + RT \ln \gamma_U)$.

fraction of the total solution volume in which it can exist.[7] Other macromolecues reduce this available volume by different amounts for folded and unfolded RNA due to the different size of these states and, therefore, change the chemical potential of each state by different amounts (Figure 1). This excluded volume effect strongly depends on the relative sizes of all species present and, due to interactions between three and higher numbers of particles, becomes highly nonlinear with concentration.[18,19] For the case of RNA folding, the excluded volume effect is expected to favor more compact structures. Second, crowders can change the activities of the ions that are the primary driver for folding in solution and the activity of the solvent (in this instance, water), which will alter transitions dependent on those components. Third, there can be some specific surface interaction between the crowder and the RNA.

Experiments have been reported on the folding of RNA molecules in solutions containing small molecules (osmolytes) such as sugars or trimethylamine-*N*-oxide (TMAO) that primarily influence folding through surface interactions.[20] All of the osmolytes studied destabilized the secondary structures of various RNAs. Some of the tertiary structures of the RNAs were also destabilized, while other tertiary structures were stabilized. These were attributed to the balance of favorable and unfavorable surface interactions of the osmolytes with the bases, sugars, and phosphates.[20] Molecular dynamics (MD) simulations qualitatively agreed with this work.[21] In addition, the MD simulations emphasized the importance of crowder size in determining the mechanism and magnitude of crowder effect.

Larger, more inert, crowders are more likely to promote entropic stabilization as a consequence of the excluded volume effect, in contrast with small osmolytes. Experimental verification of these excluded volume effects in biological macromolecules has largely come from indirect measures of compactness. For example, nonspecific polymers promote the association of ribosomal subunits[22] and also the self-cleavage of a 50 nucleotide hammerhead ribozyme.[23] More recently, ribozyme turnover was found to be accelerated by adding neutral crowding cosolutes, including polyethylene glycol (M_W = 8000).[24,25] Polyethylene glycol and Ficoll crowding agents were found to promote protein folding in solution; these last results were determined by circular dichroism spectroscopy, fluorescence correlation spectroscopy, and NMR spectroscopy.[26] SANS measurements on nonbiological polymeric molecules indicated that adding Ficoll, a highly branched polysaccharide, caused the radius of gyration (R_g) of the random coil structure of the polymer to decrease. This was pictured as a direct analogue of biological polymers in the interior of cells and showed evidence of the promotion of folding by crowders *in situ*.[27] Simulations of mechanical unfolding experiments in crowded solutions have been performed for the protein ubiquitin.[28] These confirmed that crowding increases the force needed to unfold ubiquitin and, furthermore, that this force increases as the diameter of the crowder decreases.

We investigated the $MgCl_2$ dependent folding of a 195 nt group I ribozyme derived from the pre-tRNA of the bacterium *Azoarcus*, in the presence of the crowder polyethylene glycol (PEG). This ribozyme is the smallest known self-splicing group I intron, and its stability lends itself to such studies.[29] Previous work followed the compaction of this ribozyme using small-angle X-ray (SAXS) and neutron scattering techniques.[30,31] These clearly highlighted the importance of stable 3D tertiary interactions for the two-state folding transition. Here, we use SAXS to directly monitor the collapse and folding of the ribozyme in the presence of the crowder polyethylene glycol (PEG). We found that PEG stabilizes the compact RNA, shifting midpoints of $MgCl_2$ titrations to lower concentrations. Additionally, we measure the change in water activity and show that the change in RNA stability is due to the excluded volume effect rather than perturbations to the activities of ions or water.

Experimental Methods

RNA Solution Preparation. The *Azoarcus* ribozyme (195 nt) was transcribed *in vitro* from pAz-IVS digested with *Ear*I and gel purified as previously described.[31,32] The transcription reactions (10 mL) were done in 50 mL centrifuge tubes with 5 μg/mL plasmid DNA, 2 mM of each nucleotide triphosphate, and 50000 units of T7 RNA polymerase. Reactions were incubated at 37 °C for 6 h and then concentrated to ~3 mL using Amicon Ultra-15 centrifugal filter devices (Millipore). The RNA was then purified from a

(18) Minton, A. P. *Methods Enzymol.* **1998**, *295*, 127.
(19) Boublík, T. *Mol. Phys.* **1986**, *59*, 371.
(20) Lambert, D.; Draper, D. E. *J. Mol. Biol.* **2007**, *370*, 993.
(21) Pincus, D. L.; Hyeon, C.; Thirumalai, D. *J. Am. Chem. Soc.* **2008**, *130*, 7364.
(22) Zimmerman, S. B.; Trach, S. O. *Nucleic Acids Res.* **1988**, *16*, 6309.
(23) Nashimoto, M. *Eur. J. Biochem.* **2000**, *267*, 2738.
(24) Nakano, S.-I.; Kitigawa, Y.; Karimata, H. T.; Sugimoto, N. *Nucleic Acids Symp.* **2008**, *52*, 519.
(25) Nakano, S.-I.; Karimata, H. T.; Kitigawa, Y.; Sugimoto, N. *J. Am. Chem. Soc.* **2009**, *131*, 16881.
(26) Tokuriki, N.; Kinjo, M.; Negi, S.; Hoshino, M.; Goto, Y.; Urabe, I.; Yomo, T. *Protein Sci.* **2008**, *13*, 125.
(27) Le Cour, C.; Demé, B.; Longeville, S. *Phys. Rev. E* **2009**, *79*, 031910.
(28) Pincus, D. L.; Thirumalai, D. *J. Phys. Chem. B* **2009**, *113*, 359.
(29) Tanner, M.; Cech, T. *RNA* **1996**, *2*, 74.
(30) Perez-Salas, U. A.; Rangan, P.; Krueger, S.; Briber, R. M.; Thirumalai, D.; Woodson, S. A. *Biochemistry* **2004**, *43*, 1746.
(31) Chauhan, S.; Caliskan, G.; Briber, R. M.; Perez-Salas, U. A.; Rangan, P.; Thirumalai, D.; Woodson, S. A. *J. Mol. Biol.* **2005**, *353*, 1199.
(32) Rangan, P.; Masquida, B.; Westhof, E.; Woodson, S. A. *Proc. Nat. Acad. Sci. U.S.A.* **2003**, *100* (4), 1574.

denaturing 4% polyacrylamide gel and extracted from the gel overnight in 10 mM Tris-HCl, pH 7.5, 1 mM EDTA, and 250 mM NaCl. The purified RNA was then concentrated and exchanged with 500 mM Tris-HCl and then twice more with 20 mM Tris-HCl. The resultant RNA was at 5 mg/mL, as measured from UV absorption at 260 nm; the stock was incubated at 50 °C for 5 min before use to unfold the RNA.

RNA solutions for SAXS experiments were 0.4 mg/mL in 20 mM Tris-HCl (pH 7.5) with the correct PEG concentration. RNA solution was drawn from the stock through a 1 mm capillary tube at 37 °C, passing through the X-ray beam for each measurement; the solution was kept flowing to minimize radiation damage to the RNA. Prior to each measurement, the RNA solution was incubated and stirred for 3 min at 37 °C.

SAXS. SAXS measurements were performed using the BioCAT 18ID beamline at the Argonne National Lab Advanced Photon Source. The wavelength was 1.033 Å (energy 12 keV), and measurements were made in the momentum transfer range $0.006-0.34$ Å^{-1}. SAXS data were radially averaged and corrected for background signal due to the buffer.

The scattering functions, $I(Q)$, were indirectly Fourier transformed into real space pair distribution functions of electron density, $P(r)$, using the GNOM fitting routine.[33] The radius of gyration, R_g, of the RNA molecules was then calculated from these distributions as the root-mean square of the distances of scattering points (electron density) from their weighted center. We use this as a single parameter to define the extent of the molecules, but it should be borne in mind that contributions to $P(r)$ come from a distribution of molecular sizes and shapes and, therefore, R_g also represents this distribution.

PEG has intrinsically low X-ray contrast with water[34] (0.56 mols of electrons per cm^3) allowing the measurement of RNA structure (approximately 0.93 mols of electrons per cm^3) without significant interference from the PEG. Another commonly studied large molecular crowder, Ficoll, has strong X-ray scattering which made it difficult to separate the scattering contributions due to it and RNA.

Vapor Pressure Osmometry. Vapor pressure osmometry was used in this work to measure the change in water activity due to the presence of crowders. We used a Wescor 5520 vapor pressure osmometer which operates as a dewpoint hygrometer to determine the water vapor pressure above a solution. Further details can be found in ref 35. The measured osmolality (mOsm, milliosmoles) can then be used to calculate the water activity, a_W, using the equation: $\mathrm{mOsm} = -(10^6 \ln a_W)/M_1$, where M_1 is the molecular mass of water.

Excluded Volume Calculations. The excluded volume effect, and its effect on the Gibbs free energy of different sized RNA molecules, is represented schematically in Figure 1. The activity coefficients of a probe particle (RNA) in a fluid containing a mixture of hard-particle cosolutes (PEG) can be calculated using relatively simple approximate equations of state.[18,19] From ref 18, if ρ_k is the number particle density of the kth particle species then the activity coefficient due to crowding of the ith species is

$$\ln \gamma_i = -\ln(1 - \langle\langle V\rangle\rangle) + \frac{H_i\langle\langle S\rangle\rangle + S_i\langle\langle H\rangle\rangle + V_i\langle\langle 1\rangle\rangle}{1 - \langle\langle V\rangle\rangle} + \frac{H_i^2\langle\langle S\rangle\rangle^2 + 2V_i\langle\langle H\rangle\rangle\langle\langle S\rangle\rangle}{2(1 - \langle\langle V\rangle\rangle)^2} + \frac{V_i\langle\langle H^2\rangle\rangle\langle\langle S\rangle\rangle}{3(1 - \langle\langle V\rangle\rangle)^3} \quad (1)$$

where $\langle\langle X\rangle\rangle = \sum \rho_k X_k$ and $H = R$ (particle radius), $S = 4\pi R^2$, and $V = (4\pi/3)R^3$ for spherical particles. These functions for other hard shapes are given in ref 18.

The above approach was applied to denatured biological particles, modeled as a random coil without internal excluded volume (a Brownian walk) by Minton.[36] In this approach, the effective particle for eq 1 is the convex hull of a Brownian walk, and the parameters are $H = (2/3\pi)^{1/2}h_i$, $S = (2\pi/3)h_i^2$, $V = 4(2\pi/3)^{1/2}h_i^3/27$, where h_i is the rms end-to-end distance of the ith denatured state. h_i is defined with reference to h_0, which is the equilibrium rms end-to-end distance at unit concentration and standard temperature and pressure. It takes a value of $\sqrt{6}R_g$ where R_g is the experimentally measured radius of gyration of the denatured state. A distribution of free energies associated with different h_i's are used to calculate a partition function, representing an ensemble of denatured particles, and an apparent particle activity follows from this.

From eq 1 it is noted that, in general, the smaller the crowder, the greater the chemical potential of the test particle, for a given volume fraction of crowder. This condition is clearly unphysical at some point; as the crowder gets smaller it eventually becomes indistinguishable from the solvent. We therefore multiply the crowder concentration by a factor f, which will be a function of the ratio of the radii of the crowder, R_c, with respect to the test particle, R_p, as well as the conformation of both. We know that in the limits of $R_c = 0$ and $R_c = R_p$, f should approach 0 and 1, respectively. As a first approximation, we use $f = (R_c/R_p)$.

Results

PEG Reduces R_g of Unfolded RNA. We used SAXS to measure global structural parameters of the *Azoarcus* ribozyme in solutions with varying concentrations of $MgCl_2$ and PEG to measure how the excluded volume effect changes the stability of folded RNA. Small angle scattering intensities, $I(Q)$, are shown in Figure 2 for the *Azoarcus* ribozyme in 0% and 18% wt/vol PEG1000, 20 mM Tris-HCl solution at a range of $MgCl_2$ concentrations. As the titration progresses, the intensity in the Q range $0.02-0.1$ Å^{-1} increases at higher $MgCl_2$ concentrations, indicating a compaction of the overall RNA structure. There is no significant scattering due to PEG 1000 in this Q range (not shown).

Titration curves with R_g values from Fourier transforms of the scattering data are shown in Figure 3. The measured R_g's in the completely unfolded state decrease with increasing PEG concentration, from 76 Å in 0% PEG to 64 Å in 20% PEG (% by w/v), and the R_g of the folded RNA appears to decrease in a similar fashion, but over a much smaller range, between 33 Å in 0 and 5% PEG and 29 Å in 20% PEG. The sizes of the unfolded state are larger than those determined previously[31] although the shapes of the density correlation functions are similar. This difference is due to improved statistics of the recent data, particularly in the high Q region. With improved statistics, the fitted function of $P(r)$ approaches zero at high r without any external constraint, in contrast to fits to the previous data.[31] The R_g for the folded state is close to that predicted by the crystal structure of the ribozyme, 31.1 Å.[31,37]

PEG Stabilizes Folded (Compact) State. Increased $MgCl_2$ concentrations are associated with a spatial collapse of the RNA particle, reflected in lower R_g's (Figure 3). These R_g's were fitted to an adjusted Hill equation similar to that used previously,[38] assuming that R_g decreases linearly with increasing $MgCl_2$ concentration in the unfolded state, which we observe in the low $MgCl_2$ region. This is likely due to localized Mg^{2+} ions allowing the unfolded RNA to explore configuration space with

(33) Svergun, D. *J. Appl. Crystallogr.* **1992**, *25*, 495.
(34) Thiyagarajan, P.; Chaiko, D. J.; Hjelm, R. P., Jr. *Macromolecules* **1995**, *28*, 7730.
(35) Zhang, W.; Capp, M. W.; Bond, J. P.; Anderson, C. F.; Record, M. T., Jr. *Biochemistry* **1996**, *35*, 10506.
(36) Minton, A. P. *Biophys. J.* **2000**, *78*, 101.
(37) Adams, P. L.; Stahley, M. R.; Kosek, A. B.; Wang, J.; Strobel, S. A. *Nature* **2004**, *430*, 45.
(38) Moghaddam, S.; Caliskan, G.; Chauhan, S.; Hyeon, C.; Briber, R. M.; Thirumalai, D.; Woodson, S. A. *J. Mol. Biol.* **2009**, *393*, 753.

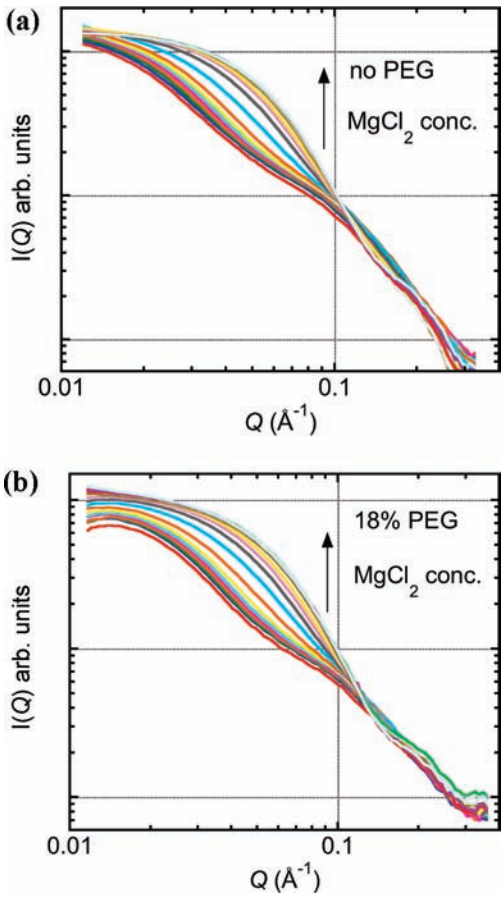

Figure 2. SAXS measurements of RNA folding. $I(Q)$ from 0.4 mg/mL *Azoarcus ribozyme* in (a) no PEG and (b) 18% PEG, plus 20 mM Tris-HCl and 0−3.13 mM $MgCl_2$. The significant increase in $I(Q)$ occurs between 0.5 and 0.81 mM $MgCl_2$ (0% PEG), and 0.14 and 0.51 mM $MgCl_2$ (18% PEG), as the RNA becomes more compact. Systematic variation at the extreme low and high Q values in (b) are due to slight beam drift during this titration, resulting in inaccurate background subtraction. This only affects the extreme Q-values, however, which were truncated in the analysis. We confirmed, using experiments where the beam had not drifted, that truncation of these data did not significantly affect the Fourier transform and the derived R_g values.

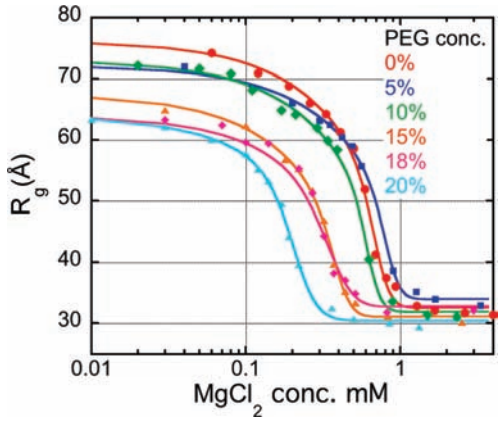

Figure 3. $MgCl_2$ titration curves of R_g values at a range of PEG concentrations. Solid lines are fits to an adjusted Hill equation (eq 2); this equation assumes a two-state model of RNA collapse and a linear decrease in R_g of the unfolded RNA with increasing $MgCl_2$ concentration. Parameters of the fits are given in Table S1. These data come from individual titration measurements; for a demonstration of their reproducibility, see the Supporting Information.

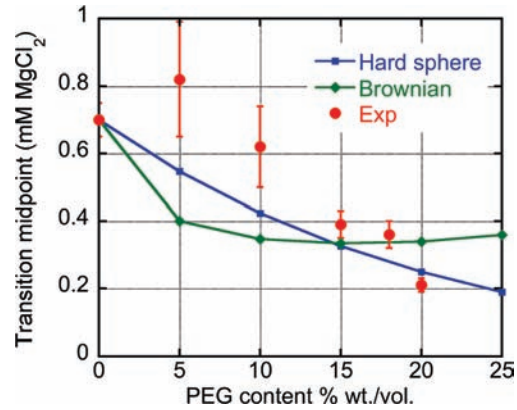

Figure 4. Midpoints of *Azoarcus* ribozyme transitions. Red symbols: experimental transition midpoints (c_m) calculated using the modified Hill equation (eq 2). Error bars represent the difference in $MgCl_2$ concentration between the data points just above and below the midpoint of the fit. Blue curve: theoretical change in transition midpoint due to excluded volume effects,[18] calculated from changes to the chemical potential assuming that both the unfolded and folded RNA are hard spheres. Green curve: same as blue curve but with unfolded particles modeled as a chain with Brownian walk statistics.

lower R_g's because of partial electrostatic screening. The use of a two-state equilibrium model for the folding transition is justified by mutational studies on *Azoarcus* ribozyme which show that the main collapse transition is due to a specific folding of the RNA.[31] According to this model, the fraction of folded RNA varies with the square of the radius and hence the Hill equation becomes

$$R_c^2 = (R_{U,0} - kc)^2 - \frac{c^n}{c_m^n + c^n}\left[(R_{U,0} - kc)^2 - R_F^2\right] \quad (2)$$

in which R_c is the radius of gyration at Mg^{2+} concentration c, $R_{U,0}$ is the radius of gyration of the unfolded RNA at zero $MgCl_2$ concentration, k is a constant, c_m is the folding midpoint concentration, R_F is the radius of gyration of the folded RNA, and n is the Hill coefficient. We interpret the Hill coefficient as reflecting the dependence of the folding equilibrium on $MgCl_2$ concentration, which is related to the change in the preferential interaction coefficient of the ions with the unfolded and folded RNA.[15,39]

As seen in Figure 3, the modified Hill equation fits the data well for all of the PEG concentrations tested. The midpoint of the transition from the unfolded to native state in the absence of PEG is 0.7 mM $MgCl_2$ at 37 °C, slightly higher than that observed previously for the *Azoarcus* ribozyme at 32 °C (0.34 mM).[31]

Importantly, PEG lowered the midpoints (c_m) of the folding transitions, consistent with added stabilization of the folded RNA. The midpoint of the folding transition for RNA in 20% PEG is 0.21 mM, considerably lower than that for the solution without PEG. Apart from a small increase in c_m between 0 and 5% PEG, the transition midpoints decreased smoothly as the weight/volume fraction of PEG was increased from 5% to 20% (Figure 4). The standard state free energy change of RNA folding is calculated using $\Delta G^0 = -RT \ln(K^0)$, where $K^0 = 1/c_m{}^n$ at the transition midpoint because the unfolded and folded RNA activities are equal. $\Delta G^0 = -2.86RT$ in the aqueous solution. The introduction of 20% PEG lowers the total folding

(39) Misra, V. K.; Draper, D. E. *J. Mol. Biol.* **2002**, *317*, 507.

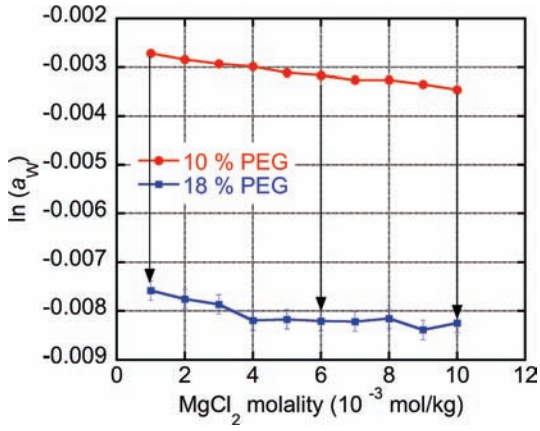

Figure 5. Water activity in PEG solutions. Measured water activity, a_W, from vapor pressure osmometry as a function of $MgCl_2$ molality in solutions containing 10 and 18% PEG. The arrows are equal length and are intended to illustrate the fact that PEG and $MgCl_2$ molality independently affect the water activity.

free energy by 5.8 k_BT, which is a large relative stabilization, in agreement with the expectation that crowding stabilizes more compact structures. This observation is in agreement with previous calculations that demonstrate large excluded volume effects for probe particles in solutions with smaller crowder particles.[18]

Ionic Activity Change Due to Crowder. Molecular crowding changes the activities of the ions and solvent, as well as that of the RNA. Therefore, we asked whether the reduction in c_m with the addition of crowders, as shown in Figure 4, is due to an increase in $MgCl_2$ activity, a_{MgCl_2}, rather than a change in the chemical potentials of the folded and unfolded RNA. This was tested using vapor pressure osmometry to measure the water activity of $MgCl_2$ solutions, and from this the $MgCl_2$ activity was determined.

Figure 5 shows the natural logarithm of water activity, ln a_W, as a function of $MgCl_2$ molality for solutions containing 10 and 18% PEG. The water activity decreases only slightly with increasing $MgCl_2$ concentration, and to the same degree in 10 and 18% PEG solutions. Hence, PEG and $MgCl_2$ contribute to the water activity independently, and independent Gibbs−Duhem relations can be written describing the effects of PEG and $MgCl_2$ on water activity. Thus, $x_w d(\ln a_w) = -x_{MgCl_2} d(\ln a_{MgCl_2})$ and the activity of $MgCl_2$ is independent of PEG concentration for a given $MgCl_2$ molality.

Neutron scattering experiments concluded that the hydration layer of Li^+ cations in concentrated solutions were unaffected by the presence of polyethylene oxide,[40] which is chemically similar to PEG. While not being conclusive, such observations tend to support our assertion that $MgCl_2$ activities are unchanged in solution by the addition of PEG.

The tirations in Figure 3 show R_g as a function of $MgCl_2$ *molarity*; for comparison with these titrations we calculated the $MgCl_2$ activities as functions of molarity for the different PEG solutions. For example, the molality of 1 mM $MgCl_2$ in 20% PEG is 20% higher than 1 mM $MgCl_2$ in 0% PEG. This corresponds to a difference in chemical potential of 3.5%, obtained by integrating the Gibbs−Duhem relation, using experimental water activities. Independently of other effects, this change in ion activity would shift the transition midpoint from 0.7 mM in aqueous solution to 0.675 mM in 20% PEG 1000. As this is much less than the experimentally observed change, we conclude that other phenomena must dominate the effect of molecular crowding on ribozyme folding.

We also measured the pH of solutions of 20 mM Tris-HCl with 0−20% PEG 1000 and found that it changes by less than 0.07 pH units. As the catalytic activities of group I ribozymes are relatively insensitive to changes in pH up to pH 10.2,[41] the change we measure is likely to have a negligible effect on the RNA's structure.

Discussion

Water Activity Change Due to Crowders. Our results show that a molecular crowder (PEG 1000) favors compact structures of the *Azoarcus* ribozyme, strongly perturbing the folding equilibrium. As this effect cannot be explained by an increase in $MgCl_2$ activity, other phenomena such as desolvation or excluded volume must contribute to the change in chemical potential due to PEG.

Next, we consider whether the activity of the water alone can drive a change in transition midpoint. It has been shown that DNA molecules become more hydrated when they form duplexes[42] and also that the inverse, dehydration, occurs with the formation of higher-order structures, such as quadruplexes,[43] or three-way junctions.[44] Moreover, the stability of these structures is altered when the water activity is changed due to the introduction of PEG as a molecular crowder. It follows, therefore, that a reduction of water activity due to molecular crowding will destabilize the RNA secondary structure but will stabilize the tertiary structure in RNA.

To quantify the number of waters that would have to be released during folding of the *Azoarcus* ribozyme to explain the change in chemical potential, we modify the analysis found in refs 42−44. The folding of an RNA molecule in a solution containing cosolute (CS, in this paper PEG) and magnesium ions (Mg^{2+}) is represented, at constant temperature and pressure, by the equation

$$\left(\frac{\partial \ln K_{obs}}{\partial \ln a_W}\right)_{T,P} = \Delta n_{Mg^{2+}}\left(\frac{\partial \ln a_{Mg^{2+}}}{\partial \ln a_W}\right)_{T,P} - \Delta n_W - \Delta n_{CS}\left(\frac{\partial \ln a_{CS}}{\partial \ln a_W}\right)_{T,P} \quad (3)$$

where Δn_x is the number of molecules of species x that are released or taken up during the transition from unfolded to folded RNA; K_{obs} is the observed equilibrium constant (ratio of folded to unfolded RNA concentrations), and the a's are the activities of the various species.

At the transition midpoints there are equal fractions of folded and unfolded RNA; hence K_{obs} is constant and the derivative on the left-hand side of eq 3 is zero. We assume that Δn_{CS} is zero; i.e. the PEG is not directly released or taken in during the folding transition. We also identify $a_{Mg}{}^{2+}$ with the midpoint concentration, c_m. With these assumptions we rearrange eq 3 to obtain

(40) Annis, B. K.; Badyal, Y. S.; Simonson, J. M. *J. Phys. Chem. B* **2004**, *108*, 2554.
(41) Tanner, M. A.; Cech, T. R. *RNA* **1996**, *2*, 74.
(42) Nakano, S.; Karimata, H.; Ohmichi, T.; Kawakami, J.; Sugimoto, N. *J. Am. Chem. Soc.* **2004**, *126*, 14330.
(43) Miyoshi, D.; Karimata, H.; Sugimoto, N. *J. Am. Chem. Soc.* **2006**, *128*, 7957.
(44) Muhuri, S.; Mimura, K.; Miyoshi, D.; Sugimoto, N. *J. Am. Chem. Soc.* **2009**, *131*, 9268.

$$\Delta n_{Mg^{2+}}\left(\frac{\partial \ln c_m}{\partial \ln a_W}\right)_{T,P} = \Delta n_W \quad (4)$$

This is the derivative of the $MgCl_2$ concentration at the folding transition midpoint (c_m) with respect to water activity, which is obtained from vapor pressure osmometry, multiplied by $\Delta n_{Mg^{2+}}$, which we assume to be identical to the value obtained from Hill analyses of the titration curves (n in eq 2). The gradient of $\Delta n_{Mg^{2+}} \ln c_m$ plotted as a function of $\ln a_W$ (Figure 6) is therefore Δn_W, the number of water molecules released during the folding transition. The value obtained from a fit to Figure 5 is 970 ± 90.

It is important to recognize that 970 molecules represents the number of water molecules that must be released to account for the free energy change of tertiary structure formation. To estimate how many water molecules could be plausibly released during the tertiary folding transition of the ribozyme, we calculated the solvent accessible surface area (SASA) using the POPS program[45,46] for the native structure[37] and for two approximations of the unfolded state. In one model of the unfolded state, we separated the native structure into its constituent helical domains, leaving all the base pairing as it is for the native state. For the second estimate, we also unpaired all the helices that are unstable at $MgCl_2$ concentrations below the main folding transition, based on nuclease probing experiments.[47]

The total SASAs are 33 900 Å^2 for the folded structure and 36 300 and 36 900 Å^2 for the lower and upper limit unfolded structures, respectively. Thus, the total surface area buried during the tertiary folding transition is approximately 2400−3000 Å^2. The number of hydrating water molecules per unit surface volume was calculated to be 0.018 Å^{-3} for tRNA, where the surface volume is taken to be a volume within 3.5 Å of the surface.[48] We assume that the surface water density for the *Azoarcus* ribozyme is the same and calculate the surface volume as the SASA multiplied by 3.5. This gives a total difference of 152 and 194 water molecules associated with the RNA surface for the lower and upper approximations, respectively, which is significantly fewer than the 970 waters predicted from the change in chemical potential of the RNA. We conclude, therefore, that the magnitude of the stabilization of the folded state that we observe is unlikely to be driven entirely by changes to the water activity due to the presence of crowders.

Excluded Volume Effects. We now consider the excluded volume effects as the origin of the change in RNA folding midpoint concentration. The difference between the activity coefficients of RNA molecules with different radii in a crowded solution can be calculated using eq 1 in the Experimental Methods section. Two sets of calculations were performed using two different approximations for the unfolded RNA. In the first, we assumed the unfolded RNA is a hard sphere. In the second, depicted schematically in Figure 1, we assumed the configuration of the unfolded chain is described by a Brownian walk. In both cases, we assumed the folded RNA and PEG are hard spherical particles. Both of these models (Brownian walk and hard sphere) are approximations to the actual RNA structure. The unfolded state is likely to be more ordered than a Brownian walk, but less ordered than a hard sphere. Nonetheless, these approximations allow us to gauge whether the excluded volume can account for the magnitude of the shift in RNA folding midpoint observed experimentally.

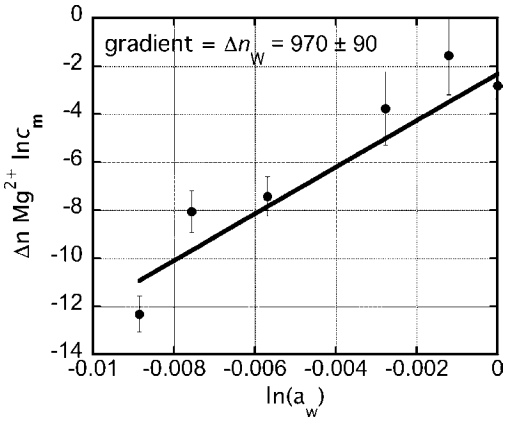

Figure 6. Change in water activity linked to RNA folding. Log of the transition midpoint $MgCl_2$ concentration (c_m) multiplied by n from eq 1, versus the log of water activity a_w obtained from vapor pressure osmometry measurements. The slope of the line represents the total number of waters Δn_w that would have to be released during folding to account for the measured perturbation to the folding free energy.

The radius of PEG 1000 was assumed to be constant across all Mg^{2+} and PEG concentrations with a value of 7.34 Å, calculated from $R_{PEG} = (3M_{PEG}\upsilon_{PEG}/4\pi N_A)^{1/3}$, in which M_{PEG} and υ_{PEG} are the molecular weight and partial specific volume of PEG, respectively. A radius of 7.34 Å is also consistent with previous neutron scattering measurements.[49]

Next, we calculate how the changes in activity coefficients of the folded and unfolded RNA shifts the transition midpoints. As shown in Figure 1, the change in standard state folding free energy upon the addition of crowder is defined to be $\Delta G^{0,C} = (G^{F,0} + RT \ln \gamma_F) - (G^{U,0} + RT \ln \gamma_U) = \Delta G^0 + RT\ \Delta\ln(\gamma)$, where γ_F and γ_U are the activity coefficients due to crowder of the folded and unfolded state, calculated according to eq 1. As can be seen in Figure 1, the light blue halos depicting excluded volume around the crowders are larger for the unfolded than the folded RNA. Hence, γ_U is larger than γ_F for a given crowder size and concentration. ΔG is related to a transition midpoint, c_m, using the identity $\Delta G = -RT \ln(1/c_m^n)$, so we can calculate the new transition midpoint due to the addition of crowder as $c_m = c_{m,0} \exp(\Delta\ln(\gamma)/n)$, where $\Delta G^0 = -RT \ln(1/c_{m,0}^n)$ and $c_{m,0}$ is the transition midpoint with no crowder. It should be noted that this approach to translating a folding energy perturbation into a shift in $MgCl_2$ concentration at the folding midpoint is equivalent to that used by Minton[36] to calculate the effect of volume exclusion on protein denaturation by urea.

For a two-state collapse between hard spheres with R_g's of 60 and 31 Å (corresponding to the experimentally measured values, just before and after the collapse transition), the predicted Mg^{2+} midpoint was 0.25 mM in 20% PEG. If the unfolded RNA is modeled by a Brownian walk with $h_i = \sqrt{6}R_g = 186$ Å (R_g in this instance is taken to be the completely unfolded state at 0% PEG, 76 Å), the predicted midpoint was 0.34 mM $MgCl_2$. The predicted midpoint changes for 0−25% PEG are compared to the experimentally measured midpoints in Figure 4.

It can be seen in Figure 4 that these simple excluded volume models correctly predict the magnitude of the RNA stabilization

(45) Fraternali, F.; Cavallo, L. *Nucleic Acids Res.* **2002**, *30*, 2950.
(46) Cavallo, L.; Kleinjung, J.; Fraternali, F. *Nucleic Acids Res.* **2003**, *31*, 3364.
(47) Chauhan, S.; Woodson, S. A. *J. Am. Chem. Soc.* **2008**, *130*, 1296.
(48) Roh, J. H.; Briber, R. M.; Damjanovic, A.; Thirumalai, D.; Woodson, S. A.; Solokov, A. P. *Biophys. J.* **2009**, *96*, 2755.
(49) Thiyagarajan, P.; Chaiko, D. J.; Hjelm, R. P., Jr. *Macromolecules* **1995**, *28*, 7730.

at 20% PEG, while the changes in water and ion activity predict a change of only a few percent. However, the shapes of the theoretical and experimental curves do not match. The experimental folding transitions change most in the higher PEG region, unlike in the models where a larger change occurs at lower PEG concentrations. The models also do not capture the small increase in c_m between 0 and 5% PEG, although this increase is barely greater than experimental uncertainty.

The difference between the theoretical and experimental curves almost certainly originates in the simplistic models (Brownian chain, sphere) used to represent RNA and PEG in the excluded volume calculations. These simplified shapes do not accurately represent the complex shape of the ribozyme and do not account for differences in the dynamics or flexibility of the folded and unfolded RNA. Further work is needed to model these effects more precisely. Nonetheless, the simple models allow us to gauge the magnitude of the excluded volume effect and determine if it is comparable to the shift in transition midpoint observed experimentally.

Given the approximations introduced in our analysis, it is encouraging that the excluded volume models describe the magnitude of the transition midpoint shift. Certainly, we find that changes in the activities of the water and ions cannot be responsible for the experimentally observed shift in the Mg^{2+} titrations. We therefore conclude that excluded volume effects are responsible for the increased stability of the folded RNA, but the simplified models outlined here do not describe the details of these effects.

Biological Significance. The natural intracellular environment is a crowded place. We have shown that this crowding significantly perturbs the free energies of RNA conformers due to the excluded volume effect, favoring structures that are more compact. Furthermore, the magnitude, direction, and qualitative nature of the crowding perturbation, as measured experimentally, can be explained with simple models describing the excluded volume. For the *Azoarcus* ribozyme in solutions containing PEG, these perturbations are responsible for a shift in the collapse transition from 0.7 to 0.21 mM $MgCl_2$ in 0% and 20% PEG solutions, respectively, or a change in folding free energy of $\sim -6\ k_BT$. For comparison, in a solution containing 0.21 mM $MgCl_2$ and 0% PEG, just 0.016% of the ribozymes are folded as opposed to 50% when 20% PEG is added.

There are several reasons why folding of the *Azoarcus* ribozyme is sensitive to the excluded volume effect of molecular crowding. First, under the low ionic strength buffer used in our experiments, the unfolded state is extended and semirigid, resulting in a large compaction of the RNA when it folds in the presence of $MgCl_2$.[30] Thus, the volumes swept out by the unfolded and folded RNAs differ dramatically, as seen in the R_g's derived from the experimental scattering data (Figure 3). Second, the entropy gained by the release of waters and co-ions from the unfolded RNA is probably much smaller than that for a protein of comparable size.[50] At the same time, entropy is lost because more counterions associate tightly with the folded RNA.[13] Therefore, changes in water activity and ion activity due to molecular crowding likely offset each other, reducing their effect on the RNA folding equilibrium.

Many domains of RNA structure are less stable than the *Azoarcus* ribozyme, requiring more than 5 mM $MgCl_2$ to fold in vitro. For such RNAs, molecular crowding may favor compact intermediates that more readily bind proteins or other ligands that stabilize their native fold. The energetic constraints placed on biomacromolecular species due to their excluded volume contribute to the functioning of, and therefore evolution of, that species. We have shown that for a noncoding ribozyme this contribution is non-negligible, and we anticipate that this result is true generally.

Acknowledgment. The authors thank Tom Irving (BioCAT), Lin Yang and Marc Allaire (NSLS X9) for assistance with SAXS experiments, D. Draper and D. Lambert for assistance with the Vapor pressure osmometry experiments, R. Behrouzi for help with sample preparation, and D Thirumalai for helpful discussions. This work was supported by NIST and a grant from the NIH (GM60819). Use of the Advanced Photon Source was supported by the U.S. Department of Energy, Basic Energy Sciences, Office of Science, under contract No. W-31-109-ENG-38. BioCAT is a National Institutes of Health-supported Research Center RR-08630. Use of the National Synchrotron Light Source, Brookhaven National Laboratory, was supported by the U.S. Department of Energy, Office of Science, Office of Basic Energy Sciences, under Contract No. DE-AC02-98CH10886.

Supporting Information Available: Figures S1 and S2 illustrate the reproducibility of the scattering data and Table S1 reports the fit parameters in Figure 3. This information is available free of charge via the Internet at http://pubs.acs.org/.

JA101500G

(50) Dill, K. A. *Biochemistry* **1990**, *29* (31), 7133.